10.1126/science.1085945

SUPPORTING ONLINE MATERIALS FOR DUEBER ET AL., DOI: 10.1126/science.1085945

MATERIALS AND METHODS

Protein construction and purification

Switch proteins. Component domains and binding motifs used for switch protein construction are listed in Table S1. Plasmids bearing these component DNA sequences were amplified by multi-step polymerase chain reaction (PCR), using primers that encoded for the appropriate intramolecular ligand motifs and linkers. All linkers were poly –Ser-Gly- repeats. Proteins were expressed as fusions to either a cleavable hexa-histidine tag (pET19-derived vector) (*S1*) or glutathione S-transferase (GST) (pGEX4T, Pharmacia) in *Escherichia coli* (BL21-DE3) as previously described (*S2*). Desired protein was purified by chromatography on Ni-NTA resin (Qiagen) or glutathione-agarose resin (Sigma). In the case of polyhistidine tagged proteins, the affinity tag was removed by incubation with tobacco etch virus (TEV) protease at 25°C for 2 hrs, after which the reaction mixture was passed over a second Nickel-NTA column. Proteins were further purified using Source S or Q columns (Pharmacia).

Cdc42. A soluble fragment of human Cdc42 (residues 1-179) for use as an input molecule was expressed in *Escherichia coli* (BL21-DE3) as a polyhistidine fusion, and

purified as described above for switch proteins. Purified Cdc42 was activated by incubating with 10 fold excess of GTPγS for 15 min at 30 °C, followed by addition of 50 fold excess $MgCl_2$ to quench the reaction. Charged Cdc42 was dialyzed in 50 mM KCl, 1 mM $MgSO_4$, 1 mM EGTA, and 10 mM imidazole (pH 7.0).

Peptide Synthesis. Peptides were synthesized using conventional solid-phase Fmoc-amino acid chemistry. SH3 and PDZ domain ligand peptides were synthesized on Rink-Amide resin (Novabiochem) and Wang resin (Novabiochem), respectively. All peptides were N-terminally acetylated, cleaved, and purified as described (*S3*). SH3-peptide affinities were previously measured (*S4-S6*), while PDZ-binding affinities were measured by competition with dansylated-peptide as described (*S3*).

Actin Polymerization Assays

Reagent preparation. Actin was purified from rabbit muscle, as described (*S7*). Rabbit skeletal muscle actin was pyrene-labeled as described (*S8*). Arp2/3 was purified from bovine brain by a two-step purification scheme adapted from (*S9*). Briefly, brains were homogenized in an equal volume of buffer (50 mM PIPES (pH 6.8), 5 mM EGTA, 2 mM $MgCl_2$, 1 mM DTT, 0.1 PMSF, and 0.2 mM ATP) using a blender (Waring). Insoluble materials were separated by centrifugation and the supernatant was incubated with SP-sepharose (Amersham). Fractions eluted with the above buffer + 100 mM KCl were applied to an affinity column composed of GST-tagged human WASP residues 418-502. Arp2/3 was eluted with 200 mM $MgCl_2$, 150 mM NaCl, 0.2 mM ATP, 1 mM DTT, 10mM imidazole (pH 7.5). Fractions containing protein were pooled and the concentration of $MgCl_2$ reduced to 0.2 mM by dialysis.

Pyrene Actin Polymerization Assay. Actin polymerization assays were performed essentially as previously described (*S10*) with modifications for use of a SpectraMax Gemini XS (Molecular Devices) fluorescent plate reader (excitation: 365 nm; emission: 407 nm). Briefly, a solution consisting of 10% pyrene-labeled actin was converted from a Ca-ATP to a Mg-ATP form by addition of $MgCl_2$ and EGTA to final concentrations of 50 µM and 200 µM, respectively. This solution was incubated at 25°C for 10 min in a 96 half area well plate (Corning)(10 µl per well). To initiate polymerization, the solution containing Arp2/3, switch construct, and appropriate ligand preincubated for 10 min at 25°C was added to the actin mix. Final assay conditions were 1.3 µM actin, 5 nM Arp2/3, 50 nM switch, 50 mM KCl, 1 mM $MgSO_4$, 1 mM EGTA, 0.2 mM ATP, 1 mM DTT, 3 µM $MgCl_2$, and 11.5 mM imidazole (pH 7.0) in a volume of 150 µl.

Raw fluorescence values from pyrene actin polymerization assays were normalized relative to lower and upper baselines using the equation $(F_{data}-F_{low})/(F_{high}-F_{low})$, where F_{data} is the fluorescence for each time point and F_{low} and F_{high} are average fluorescence obtained at the lower and upper baselines, respectively. Reaction half-time ($t_{1/2}$) is defined as the time required to reach 50% polymerization. A simple metric for relative activity was based on the experimentally measured halftime (see Fig. S1): relative activity = $(t_{1/2}^{max} - t_{1/2})/(t_{1/2}^{max} - t_{1/2}^{min})$ where $t_{1/2}^{max}$ is the halftime observed with no activator (roughly equivalent to spontaneous actin polymerization; approx. 2000 sec.) and $t_{1/2}^{min}$ is the halftime observed with the constitutively active output domain (approx. 400 sec. for output A and 600 sec. for output B). Relative activity was always

calculated using values for $t_{1/2}$, $t_{1/2}^{min}$, and $t_{1/2}^{max}$ measured simultaneously (same 96-well plate and reagents). An alternative metric for activity was the rate of actin polymerization (fluorescence units/sec) at half-polymerization.

Classification of switch behavior. Proteins from the 2-input switch library were screened for relative activity under a set of standard input concentrations: chimeric switches - no activators, 10 μM Cdc42-GTPγS, 200 μM PDZ lig, or both; heterologous switches – no activators, 200 μM PDZ ligand, 10 μM SH3 ligand, or both. These concentrations were arbitrarily chosen to be 20-100-fold higher than the K_d for the interaction of the input molecule with the isolated recognition domain. Switches were divided into behavioral classes shown in Fig. 2c based on relative activation under these conditions. Definitions for the classes are given in Fig. S4.

Modeling of switch behavior. See Fig. S5.

Bead actin polymerization assay. Spatial control of actin polymerization was assayed as follows. Carboxylated 2 μm polystyrene beads (Polysciences) were coated with GST-input fusions as described (*S11*). Briefly, 2 μm carboxylated polystyrene beads (2 μl of 2.5% slurry) were incubated in solution containing saturating amounts of GST-input fusion, mixed at the desired percentage with GST alone (no fusion), at a total protein concentration of 2 mg/ml in a volume of 160.5 μl. Beads were incubated with either 69.5 μM of monovalent ligand (GST-SH3 or GST-PDZ) or 34.8 μM of bivalent ligand (GST-SH3-PDZ). After incubation at room temperature for 1 hr, beads were pelleted and washed in XB buffer (100 mM KCl, 0.1 mM $CaCl_2$, 2 mM $MgCl_2$, 5 mM EGTA, 10 mM K•Hepes, pH 7.7). Washed beads were resuspended in 30 μl of XB. 0.5 μl of this bead solution was incubated with 1.18 μl of a 525 μM stock of soluble H14

protein for 15 min at 25 °C, then supplemented with 4.5 µl of ~30 mg/ml *Xenopus* extract (generously donated by C. Co and J. Taunton) and 0.25 µl rhodamine-labeled actin prepared as previously described (*S12*). After incubation for 5 minutes at 25 °C, a 1 µl aliquot was removed and sealed between a microscope slide and a 18 mm square coverslip with vaseline:lanolin:paraffin (at 1:1:1). After a further 5 min incubation, beads were observing with an Olympus 1X70 microscope equipped with bright-field and epifluorescent optics. Images were acquired with a Photometrics Cool Snap HQ camera (standard rhodamine filter set). Rhodamine and bright-field images were analyzed identically for each sample using Adobe Photoshop.

Table S1. Components used in switch construction and their properties.

Intramolecular ligand affinities for partner domains are reported as measured *in trans*.

Output	***Source***	***Residues***		***Ref.***
Output A	rat N-WASP	392-501		(*S13*)
Output B	rat N-WASP	429-501		(*S14*)
Regulatory Domains	***Source***	***Residues***		***Ref.***
PDZ	Mouse α-syntrophin (syn)	77-171		(*S15*)
GBD	rat N-WASP	196-274		(*S16*)
SH3	mouse Crk	134-191		(*S17*)
Intramol. ligands	***Sequence***	***Partner***	***Kd (μM)***	***Ref.***
PDZ lig. H[1]	GVKESLV	Syn PDZ	8	(*S3*), This work
PDZ lig. M[1]	GVKQSLL	Syn PDZ	100	This work
PDZ lig. L[1]	GVKESGA	Syn PDZ	1000	This work
SH3 lig. H	PPPVPPRR	Crk SH3	10	(*S18*)
SH3 lig. M	PPAIPPRQPT	Crk SH3	100	(*S6*)
SH3 lig. L	GPPVPPRQST	Crk SH3	700	(*S6*)
Output (C helix)	Rat N-WASP residues 461-479 (within Output A and B)	GBD	1	(*S2*)
Input Ligands	***Sequence***	***Partner***	***Kd (Um)***	***Ref.***
PDZ lig.	Ac -YVKESLV-COOH	Syn PDZ	8	(*S3*), This work
SH3 lig.	Ac -PPPALPPKRRR-CONH2	Crk SH3	0.1	(*S4*)
Cdc42-GTPγS	Residues 1-179	GBD	0.1	(*S2*)

[1]Affinities measured with a peptides with an N-terminal tyrosine replacing the glycine to accurately measure peptide concentration. PDZ peptides were synthesized with a N-terminal acetyl group and a C-terminal carboxyl group.

Supporting References

S1. B. J. Hillier, K. S. Christopherson, K. E. Prehoda, D. S. Bredt, W. A. Lim, *Science* **284**, 812-5 (1999).
S2. K. E. Prehoda, J. A. Scott, R. D. Mullins, W. A. Lim, *Science* **290**, 801-6 (2000).
S3. B. Z. Harris, B. J. Hillier, W. A. Lim, *Biochemistry* **40**, 5921-30 (2001).
S4. G. Posern *et al.*, *Oncogene* **16**, 1903-12 (1998).
S5. J. T. Nguyen *et al.*, *Chem Biol* **7**, 463-73 (2000).
S6. B. S. Knudsen *et al.*, *EMBO J* **14**, 2191-8 (1995).
S7. J. D. Pardee, J. A. Spudich, *Methods Enzymol* **85 Pt B**, 164-81 (1982).
S8. S. MacLean-Fletcher, T. D. Pollard, *Cell* **20**, 329-41 (1980).
S9. C. Egile *et al.*, *J Cell Biol* **146**, 1319-32 (1999).
S10. L. M. Machesky *et al.*, *Proc Natl Acad Sci U S A* **96**, 3739-44 (1999).
S11. L. A. Cameron, M. J. Footer, A. van Oudenaarden, J. A. Theriot, *Proc Natl Acad Sci U S A* **96**, 4908-13 (1999).
S12. J. Taunton *et al.*, *J Cell Biol* **148**, 519-30 (2000).
S13. R. Rohatgi *et al.*, *Cell* **97**, 221-31 (1999).
S14. J. Zalevsky, L. Lempert, H. Kranitz, R. D. Mullins, *Curr Biol* **11**, 1903-13 (2001).
S15. J. Schultz *et al.*, *Nat Struct Biol* **5**, 19-24 (1998).
S16. A. S. Kim, L. T. Kakalis, N. Abdul-Manan, G. A. Liu, M. K. Rosen, *Nature* **404**, 151-8 (2000).
S17. X. Wu *et al.*, *Structure* **3**, 215-26 (1995).
S18. J. T. Nguyen, C. W. Turck, F. E. Cohen, R. N. Zuckermann, W. A. Lim, *Science* **282**, 2088-92 (1998).
S19. Prehoda, K.E., Lim, W.A., Curr. Opin. Cell. Biol. 14, 149-54 (2002).
S20. R. D. Mullins, L. M. Machesky, *Methods Enzymol* **325**, 214-37 (2000).

Supporting Figure 1.

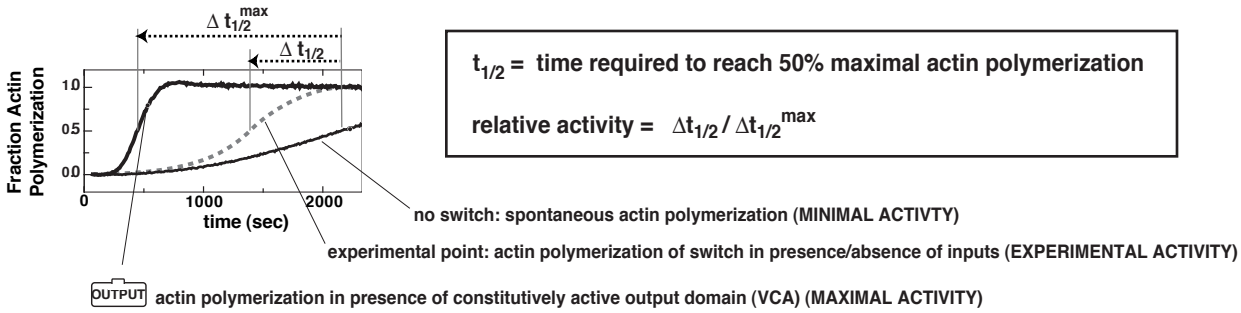

Fig. S1. Metric for relative activity of N-WASP switches based on half-time of actin polymerization. Activity of switch proteins was determined using a fluorescence-based actin polymerization assay (20, and "Methods"). Time required to reach 50% polymerization ($t_{1/2}$) was used as a metric for activity. Minimal activity was defined as the $t_{1/2}$ observed with spontaneous actin polymerization under these conditions in the presence of Arp2/3 but no nucleation promoting factors. Maximal activity was defined as the $t_{1/2}$ in the presence of the isolated output domain. Relative activities of individual constructs were scored by measuring the change in $t_{1/2}$ relative to the difference between maximum and minimum activities.

Supporting Figure 2.

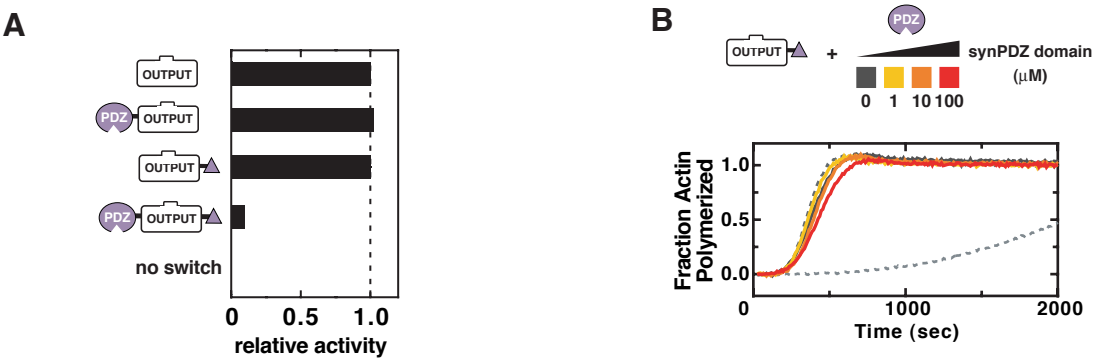

Fig. S2. Autoinhibition of synthetic single input switch requires intact intramolecular PDZ domain-ligand interaction. A. Control constructs containing the N-WASP output domain fused to either the PDZ domain or ligand alone did not exhibit significant repression (equal activity to output domain alone). Repression is only observed when both PDZ domain and ligand are fused to the output. B. Construct bearing the N-WASP output domain fused only to the PDZ ligand did not exhibit repression by PDZ domain added in trans, even when added at saturating concentrations (>10 fold above the Kd).

Supporting Figure 3.

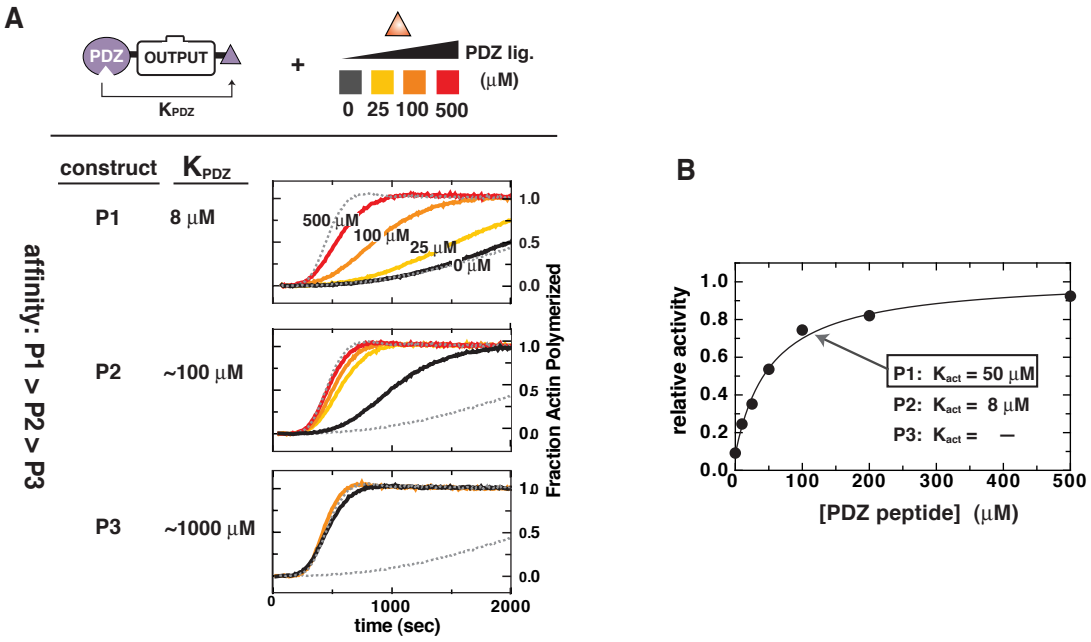

Fig. S3. Dependence of single input switch behavior on affinity of autoinhibitory ligand. **A**. Three different affinity PDZ domain/ligand pairs where examined within the same single input synthetic switch architecture. Reduced affinity of this autoinhibitory ligand resulted in reduced basal repression. **B**. Titration of free PDZ ligand (K_{PDZ} = 8 μM) relieved activity in a manner consistent with a single-ligand binding event. Reduced affinity of the autoinhibitory ligand resulted in increased switch sensitivity to free ligand. Activity is measured as in Fig. S1.

Supporting Figure 4.

Poorly Repressed:
Relative activity >0.5 under all input conditions

Insensitive:
Relative activity <0.5 under all input conditions

Single Input:
One input is an activator; other input has no effect

Negative dual input:
one input is activator; other input is repressor

Positive dual input:
both inputs are activators

~OR:
inputs either individually or in combination yield approx. equivalent level of activation

~AND:
inputs in combination yield much stronger activation than individually

Intermed:
remaining positive dual input switches

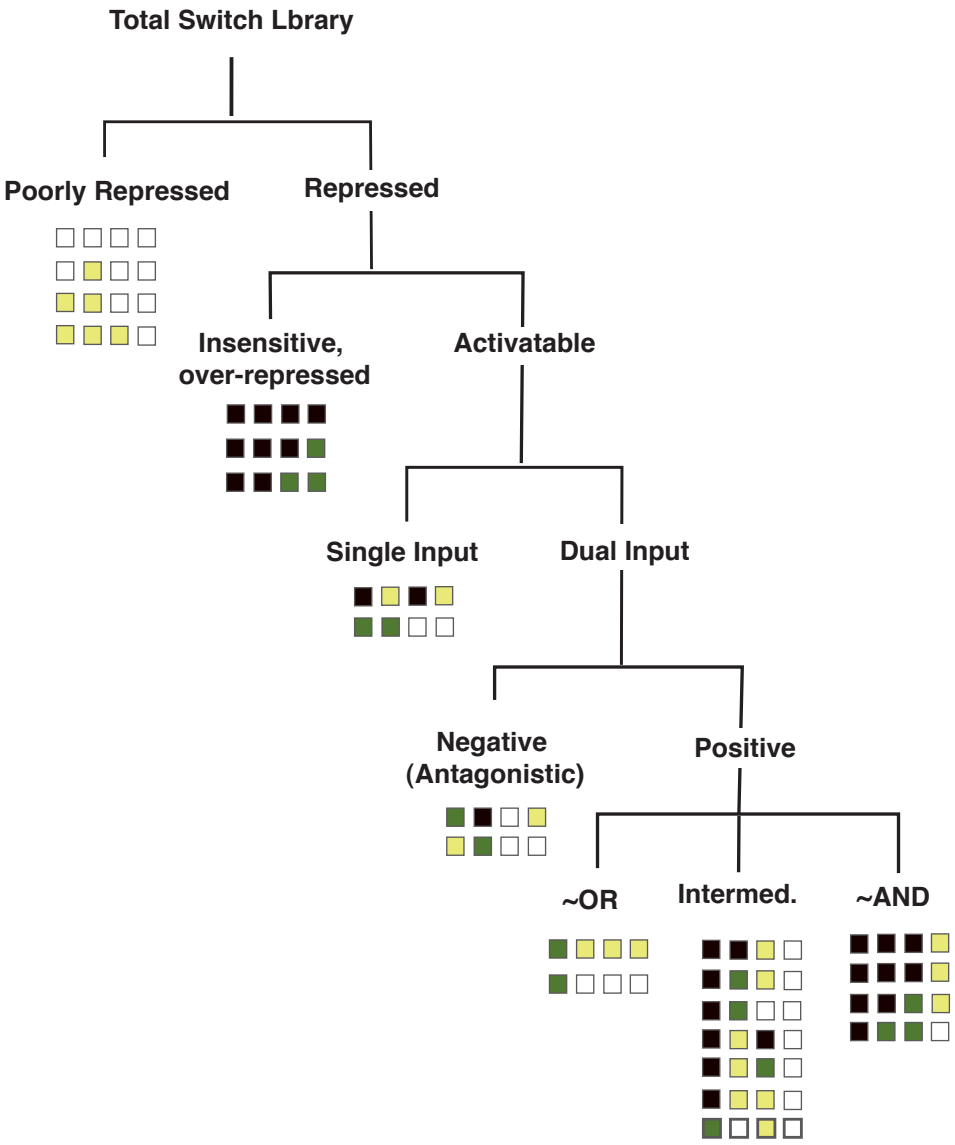

All experimentally observed switch profiles are classified above. Color code relative actiivty levels are defined in Fig. 2.

Fig. S4. Switch behavior class definitions and examples from two-input library. All experimentally observed switch profiles shown in Fig. 2 are classified above in addition to definitions used for each of these behavior classes.

Supporting Figure 5.

Fig. S5. Modeling of two input switch behavior. A. Framework for switch modeling related as equilibria describing two-input switch states and effect of ligand binding. **B**. Modeling of specific cases including AND-gates and antagonistic switches.

A. Framework for switch modeling

Equilibria describing two-input switch states and effect of ligand binding:

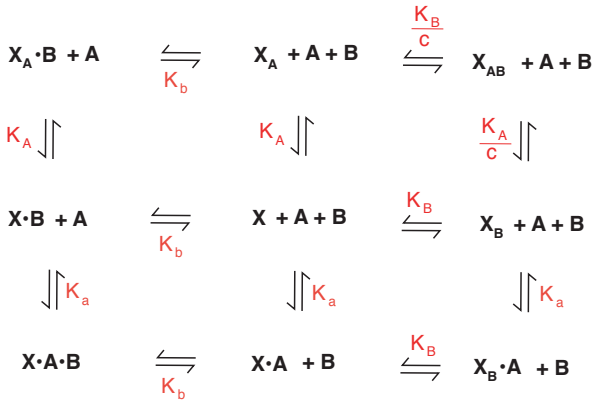

$$X_A = \frac{X}{K_A} \qquad X_B = \frac{X}{K_B} \qquad X_{AB} = \frac{X_B}{\frac{K_A}{c}} = \frac{c\,X}{K_A K_B}$$

$$X \cdot A = \frac{X\ A}{K_a} \qquad X \cdot B = \frac{X\ B}{K_b} \qquad X \cdot A \cdot B = \frac{X \cdot A\ B}{K_b} = \frac{X\ A\ B}{K_a K_b}$$

$$X_A \cdot B = \frac{X \cdot B}{K_A} = \frac{X\ B}{K_A K_b} \qquad X_B \cdot A = \frac{X \cdot A}{K_B} = \frac{X\ A}{K_a K_B}$$

Switch States:

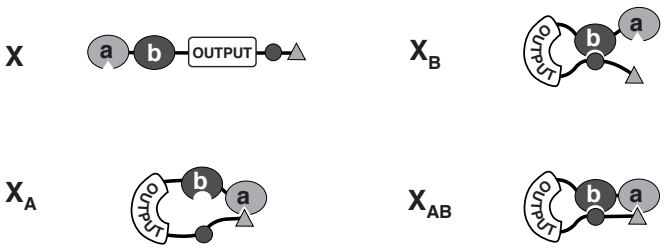

A and B are external ligands for domains a and b, respectively

Constants:

K_A , K_B **: "dissociation" constant for intramolecular binding by domain a or b, respectively. This term encompasses both the inherent affinity of the isolated domain for ligand and their effective concentration within the intramolecular context.**

K_a , K_b **: dissociation constant for intermolecular ligand binding to domain a or b, respectively.**

c **: effective concentration linking intramolecular binding of domain a with intramolecular binding of domain b; i.e. fold change in intramolecular association of one domain when the other is already engaged in intramolecular interaction.**

B. Modeling specific cases

Specific cases are modeled below, including AND-gates and antagonistic switches.

There are two extreme models that generate AND-gate like behavior (Prehoda & Lim, Supp. Ref. 18). In model I, both intramolecular interactions are required for repression (i.e. states with single intramolecular interaction are fully active). However, the two intramolecular interactions are highly cooperative (c high). Thus, in ligand mediated activation, the two intermolecular ligands act in a highly cooperative manner. In model II, the states with single intramolecular interactions are also inactive. Thus, in the absence of cooperativity both inputs are required for full activation. Many other intermediate models (i.e. hybrids of the two extremes; partial activity of single intramolecular states, etc.) are possible and also yield general AND-gate-like behavior.

i. "AND-gate," model I - highly cooperative:

- c is large
- only X_{AB} is inactive (shaded); remaining states of X are active (white)

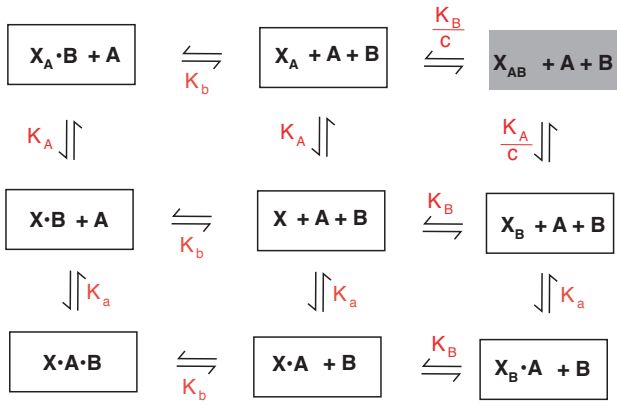

$$\text{Rel. Act.} = \frac{X + X{\cdot}A + X{\cdot}B + X{\cdot}A{\cdot}B + X_A + X_A{\cdot}B + X_B + X_B{\cdot}A}{X + X{\cdot}A + X{\cdot}B + X{\cdot}A{\cdot}B + X_A + X_A{\cdot}B + X_B + X_B{\cdot}A + X_{AB}}$$

$$= \frac{1 + A' + B' + A'B' + 1/K_A + B'/K_A + 1/K_B + A'/K_B}{1 + A' + B' + A'B' + 1/K_A + B'/K_A + 1/K_B + A'/K_B + c/K_A K_B} \qquad (A' = A/K_A\ ;\ B' = B/K_B)$$

$K_A = K_B = 0.05\ \mu M$

$c = 300$

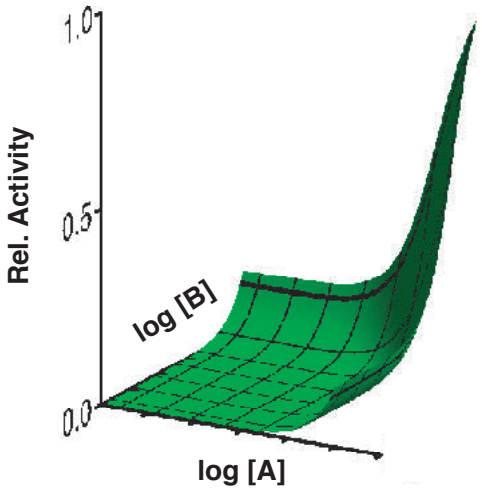

II. "AND-gate," model II semi-cooperative switch:

• X_A, X_B, and X_{AB} are inactive (shaded); only X is active (white)

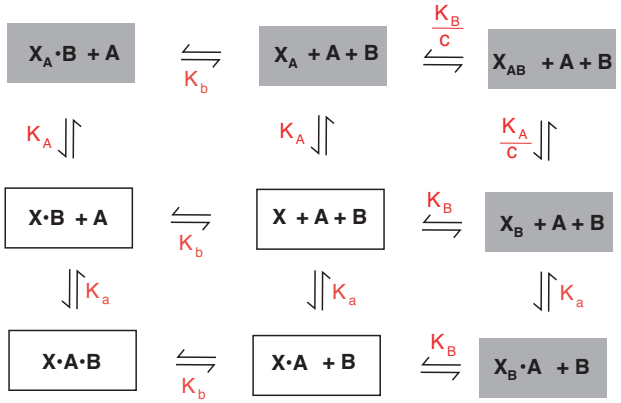

$$\text{Rel. Act.} = \frac{X + X{\cdot}A + X{\cdot}B + X{\cdot}A{\cdot}B}{X + X{\cdot}A + X{\cdot}B + X{\cdot}A{\cdot}B + X_A + X_A{\cdot}B + X_B + X_B{\cdot}A + X_{AB}}$$

$$= \frac{1 + A' + B' + A'B'}{1 + A' + B' + A'B' + 1/K_A + B'/K_A + 1/K_B + A'/K_B + c/K_A K_B}$$

$(A' = A/K_A;\ B' = B/K_B)$

$K_A = K_B = 0.05\ \mu M$

$c = 1$

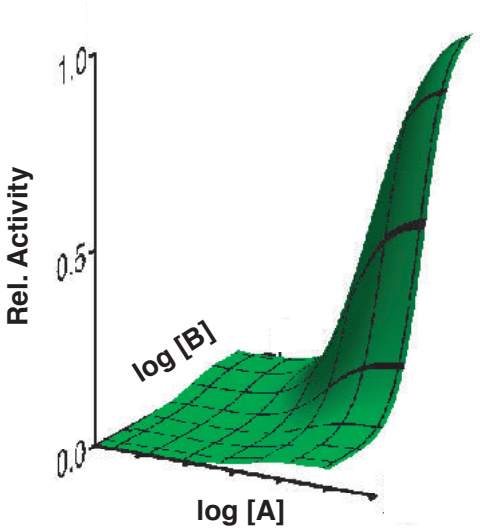

iii. Antagonistic switch:

- **c ~ 0 (anticooperative intramolecular interactions); X_{AB} state is unoccupied**
- **only X_A is inactive (shaded); X and X_B are active (white)**

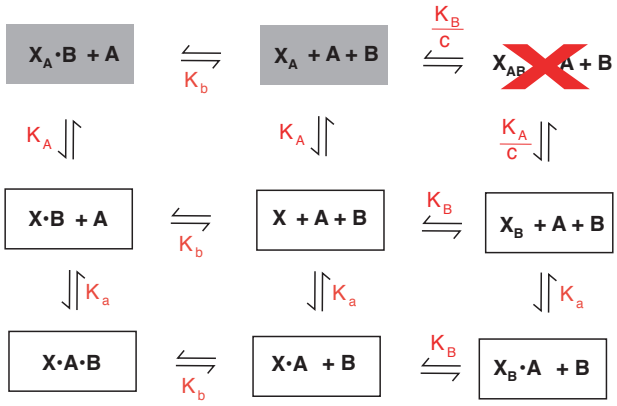

$$\text{Rel. Act.} = \frac{X + X{\cdot}A + X{\cdot}B + X{\cdot}A{\cdot}B + X_B + X_B{\cdot}A}{X + X{\cdot}A + X{\cdot}B + X{\cdot}A{\cdot}B + X_B + X_B{\cdot}A + X_A + X_A{\cdot}B}$$

$$= \frac{1 + A' + B' + A'B' + 1/K_B + A'/K_B}{1 + A' + B' + A'B' + 1/K_B + A'/K_B + 1/K_A + B'/K_A} \qquad (A' = A/K_A;\ B' = B/K_B)$$

$K_A = K_B = 0.05\ \mu M$

$c \sim 0$

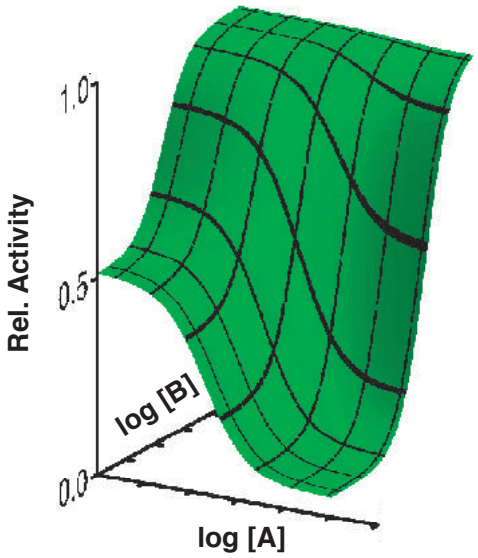

(graph shown in Fig. 4D was calculated with K_A = 0.02 μM and K_B = 0.2 μM)